



ASAP Report

Reporter: Jing Chen

Supervisors: *Prof.* Tao Ye

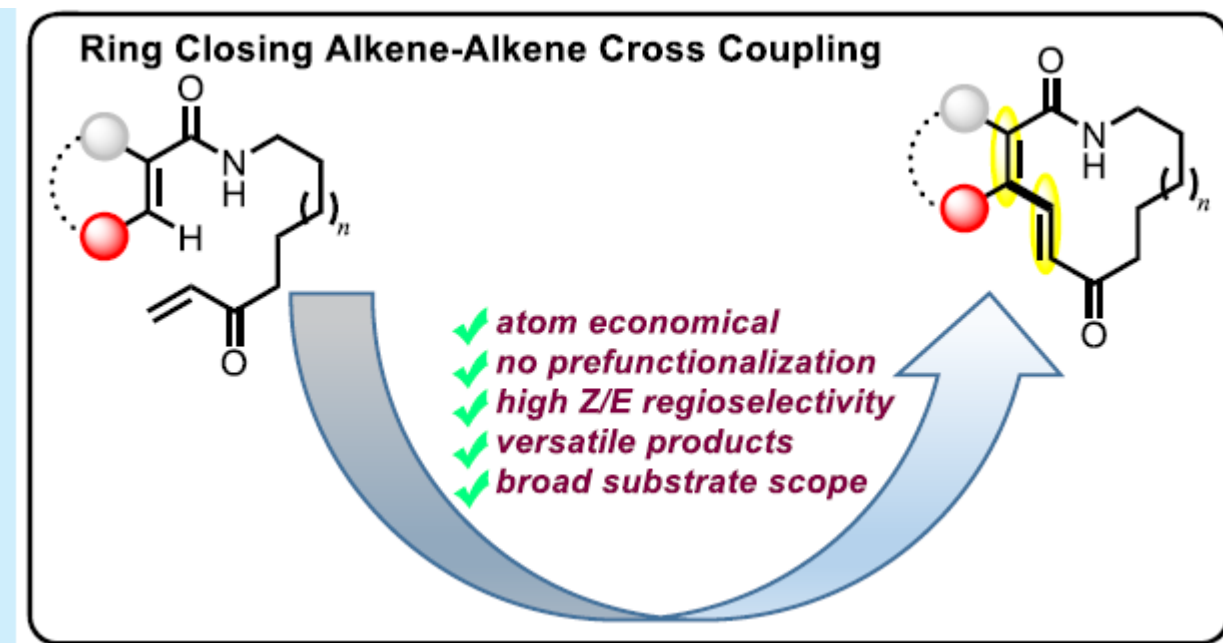
***Dr.* Yian Guo**

Dec. 7st, 2020

Introduction



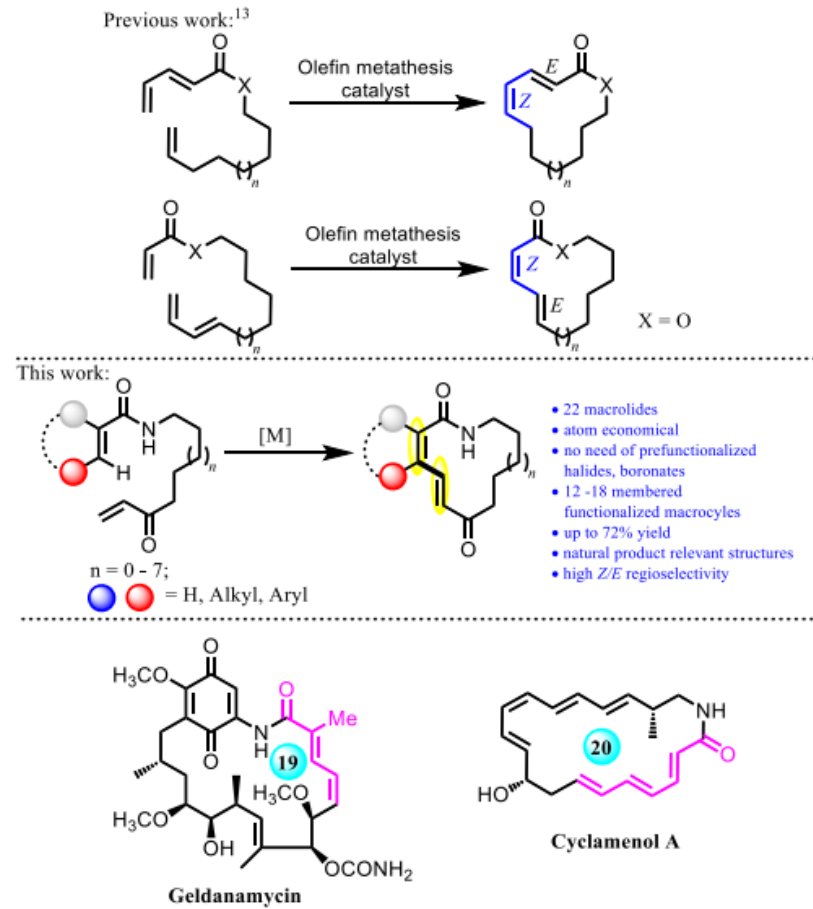
Part I : Macrolactam Synthesis via Ring-Closing Alkene–Alkene Cross-Coupling Reactions



Introduction



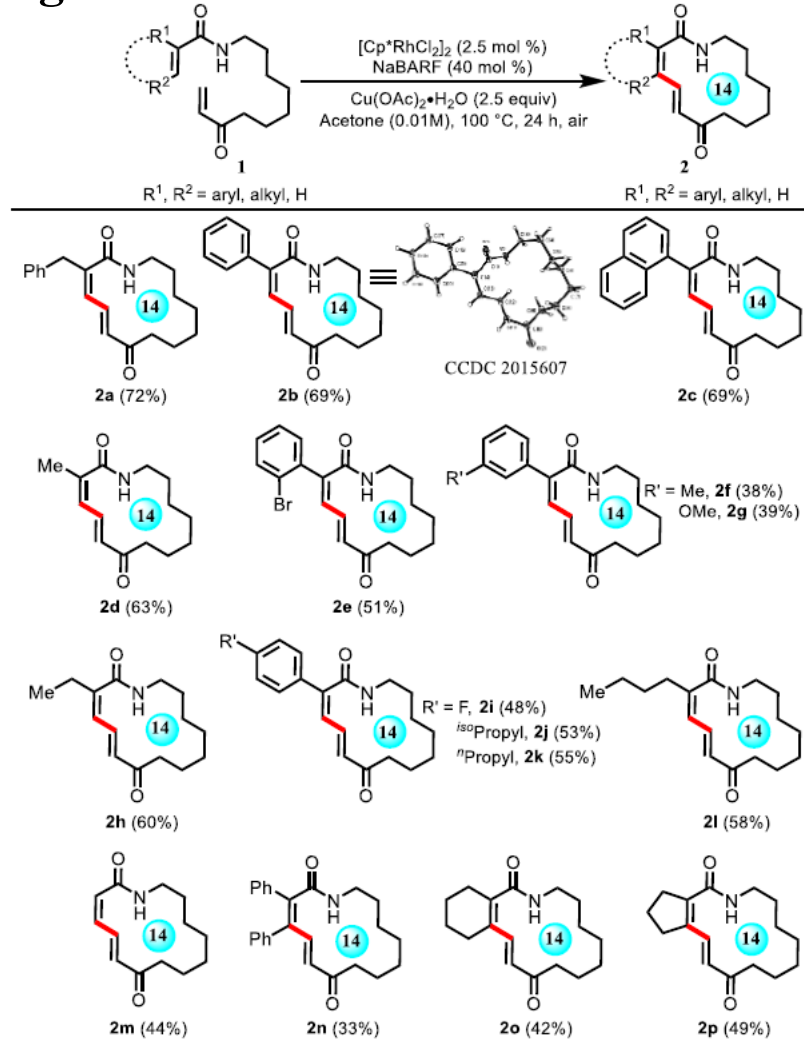
Part I : Macrolactam Synthesis via Ring-Closing Alkene–Alkene Cross-Coupling Reactions



Introduction



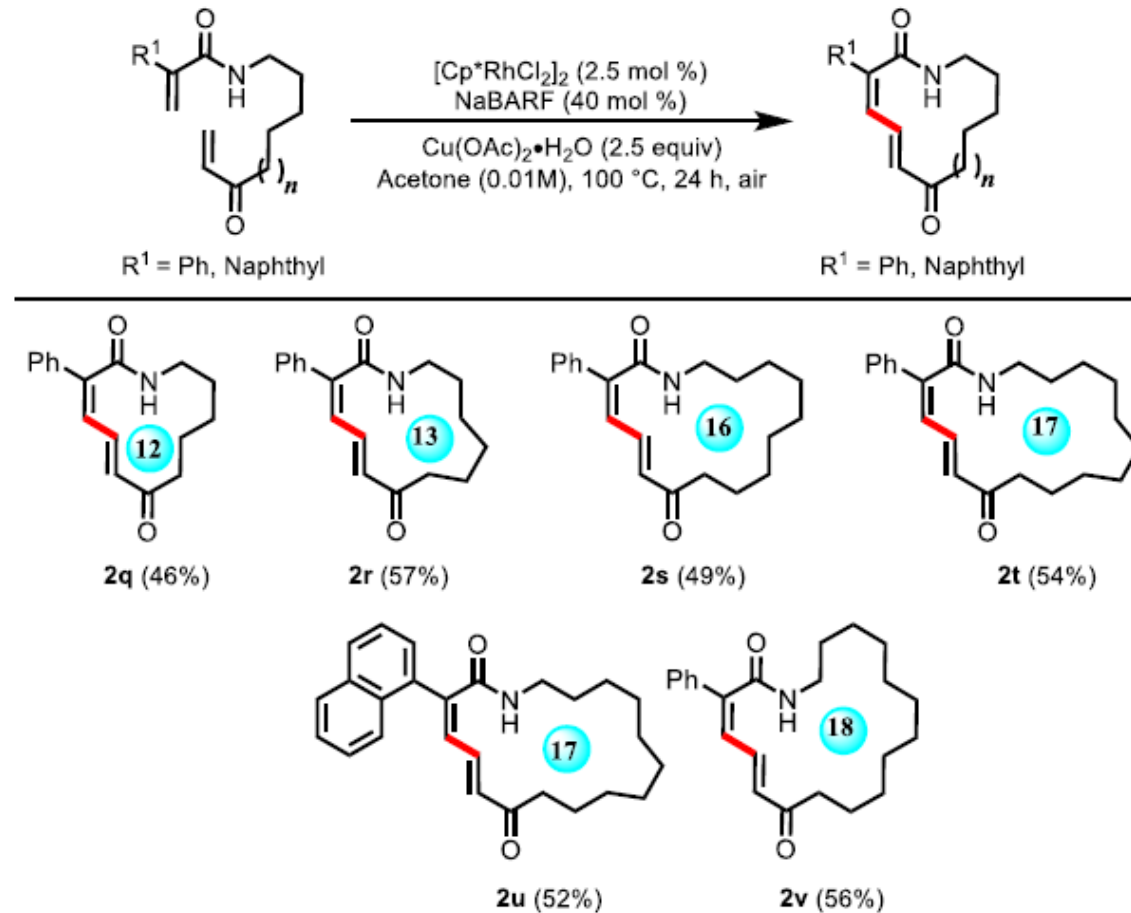
Part I : Macrolactam Synthesis via Ring-Closing Alkene–Alkene Cross-Coupling Reactions



Introduction



Part I : Macrolactam Synthesis via Ring-Closing Alkene–Alkene Cross-Coupling Reactions

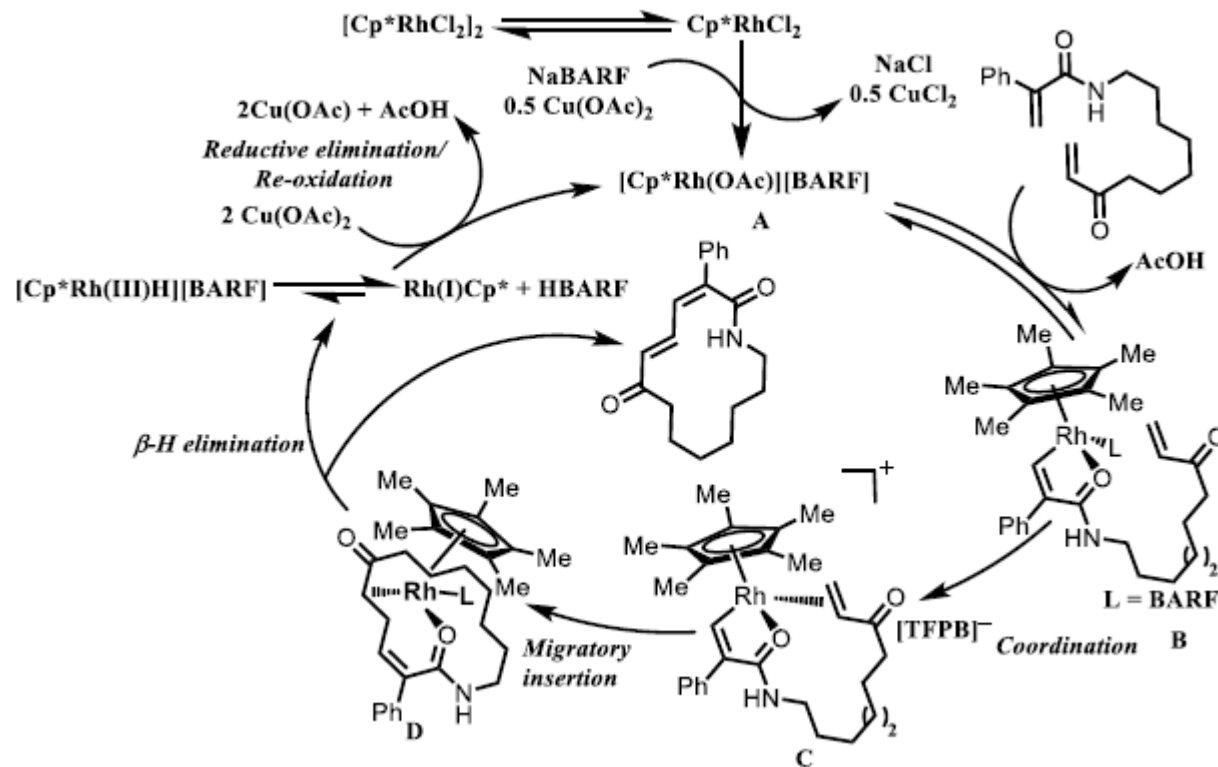


Introduction



Part I : Macrolactam Synthesis via Ring-Closing Alkene–Alkene Cross-Coupling Reactions

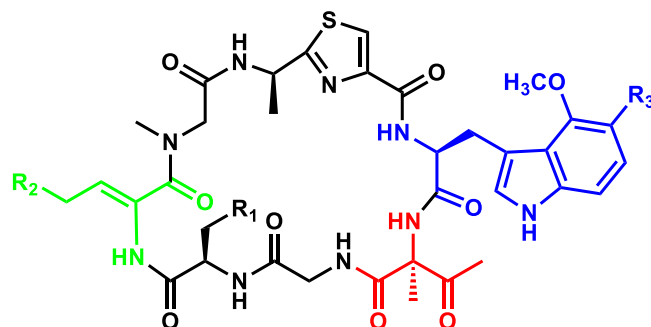
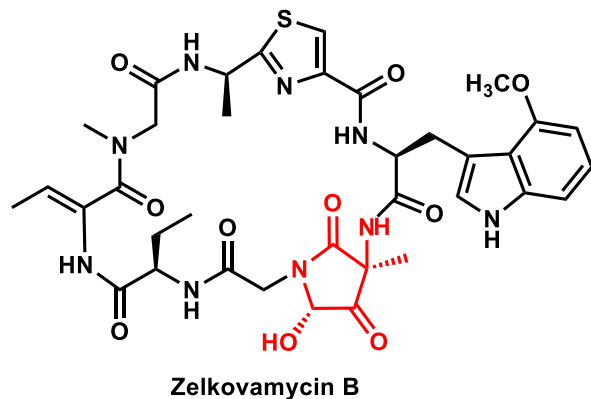
Scheme 5. Proposed Mechanism



Introduction



Part II: Zelkovamycins B–E, Cyclic Octapeptides Containing Rare Amio Acid Residues from an Endophytic *Kitasatospora* sp.



Isolation

- Four novel Cyclic Octapeptides were isolated from an endophytic *Kitasatospora* sp.

Biological activities:

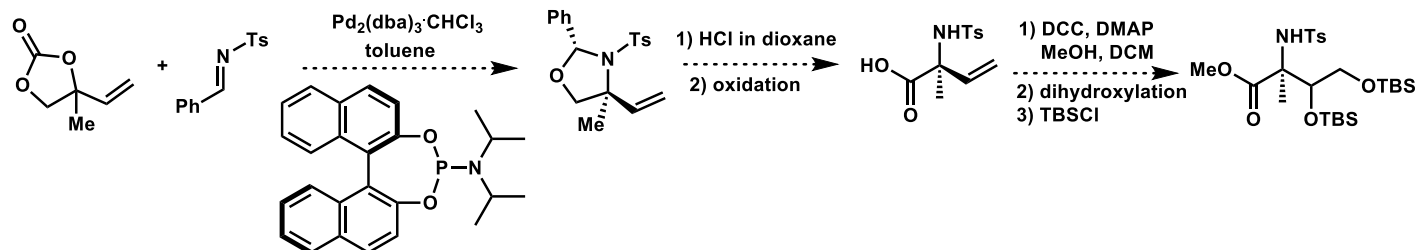
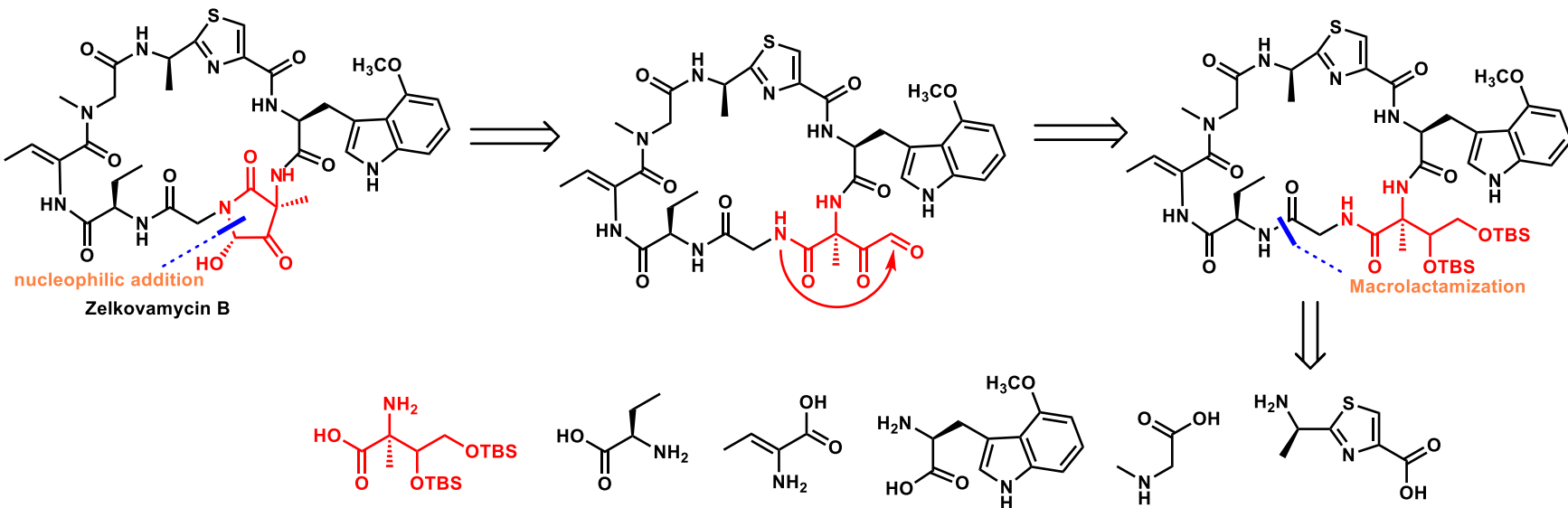
- Zelkovamycin E displayed potent inhibitory activity against H1N1 influenza A virus.

H1N1			
Compounds	EC ₅₀ (μM)	CC ₅₀ (μM)	SI
Zelkovamycin B	Not tested	>100	Not tested
Zelkovamycin C	Not tested	>100	Not tested
Zelkovamycin D	34.8±0.1	>100	>2.9
Zelkovamycin E	0.3±0.05	44.8±2.0	149
ribavirin	15.4±0.9	>100	>6.5

Introduction



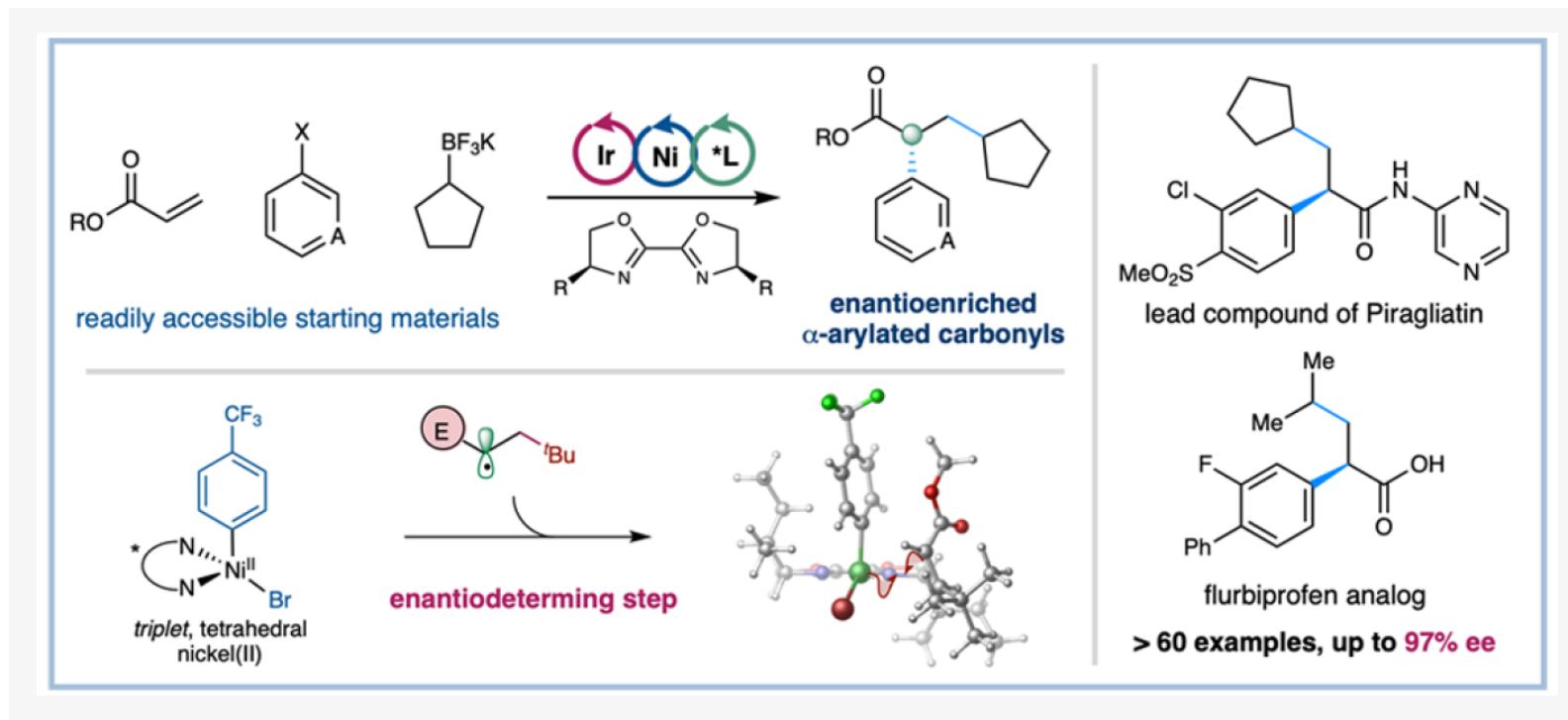
Part II: Zelkovamycins B–E, Cyclic Octapeptides Containing Rare Amio Acid Residues from an Endophytic *Kitasatospora* sp.



Introduction



Part III: General Method for Enantioselective Three-Component Carboarylation of Alkenes Enabled by Visible-Light Dual Photoredox/Nickel Catalysis



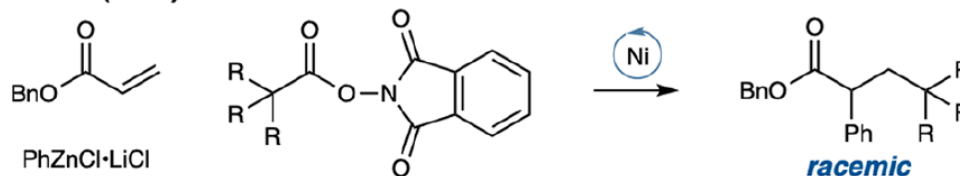
Introduction



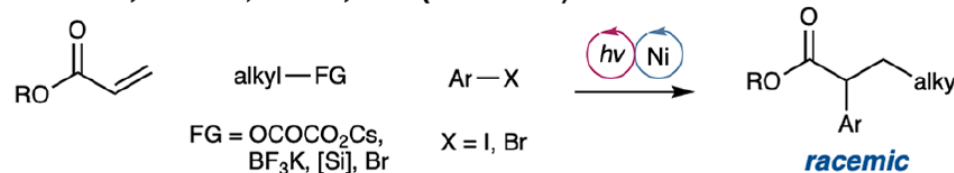
Part III: General Method for Enantioselective Three-Component Carboarylation of Alkenes Enabled by Visible-Light Dual Photoredox/Nickel Catalysis

B) Prior work on Ni-catalyzed three-component alkylarylation of acrylates

Baran (2015)

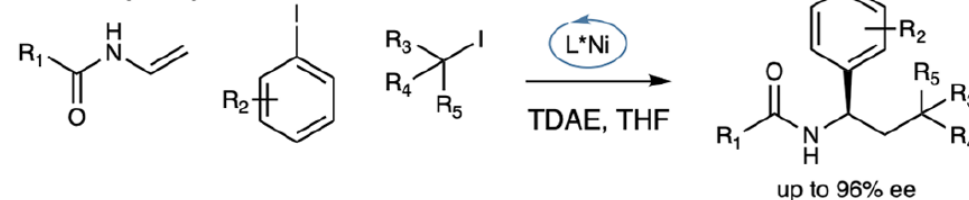


Molander, Nevado, Martin, Chu (2019-2020)



C) Prior work on enantioselective three-component alkylarylation of alkenes via Ni-catalyzed reductive coupling (Chu and Nevado)

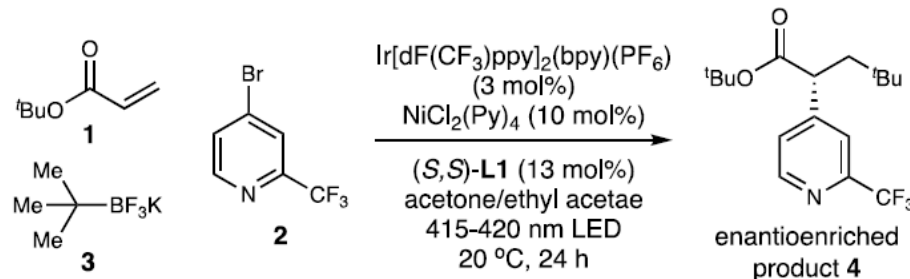
Nevado (2020)



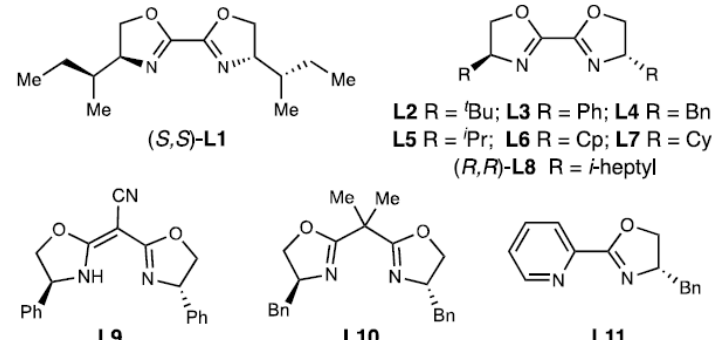
Introduction



Part III: General Method for Enantioselective Three-Component Carboarylation of Alkenes Enabled by Visible-Light Dual Photoredox/Nickel Catalysis



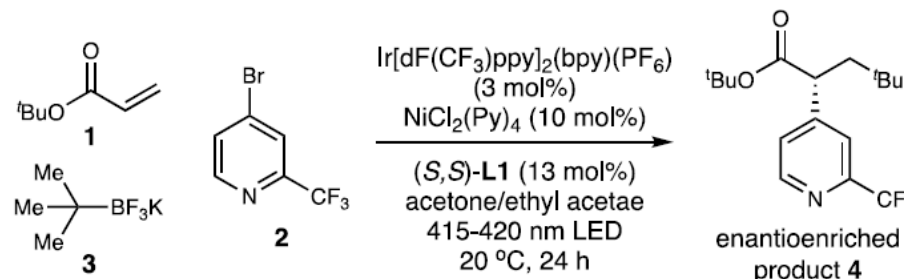
Entry	Chiral ligand	Yield	ee
1	(S,S)-L1	82%	95%
2	(S,S)-L2	21%	7%
3	(S,S)-L3	60%	86%
4	(S,S)-L4	76%	72%
5	(S,S)-L5	60%	82%
6	(S,S)-L6	83%	88%
7	(S,S)-L7	87%	88%
8	(R,R)-L8	74%	-88%
9	(S,S)-L9, (S,S)-L10, (S)-L11	5%~78%	3%~24%



Introduction

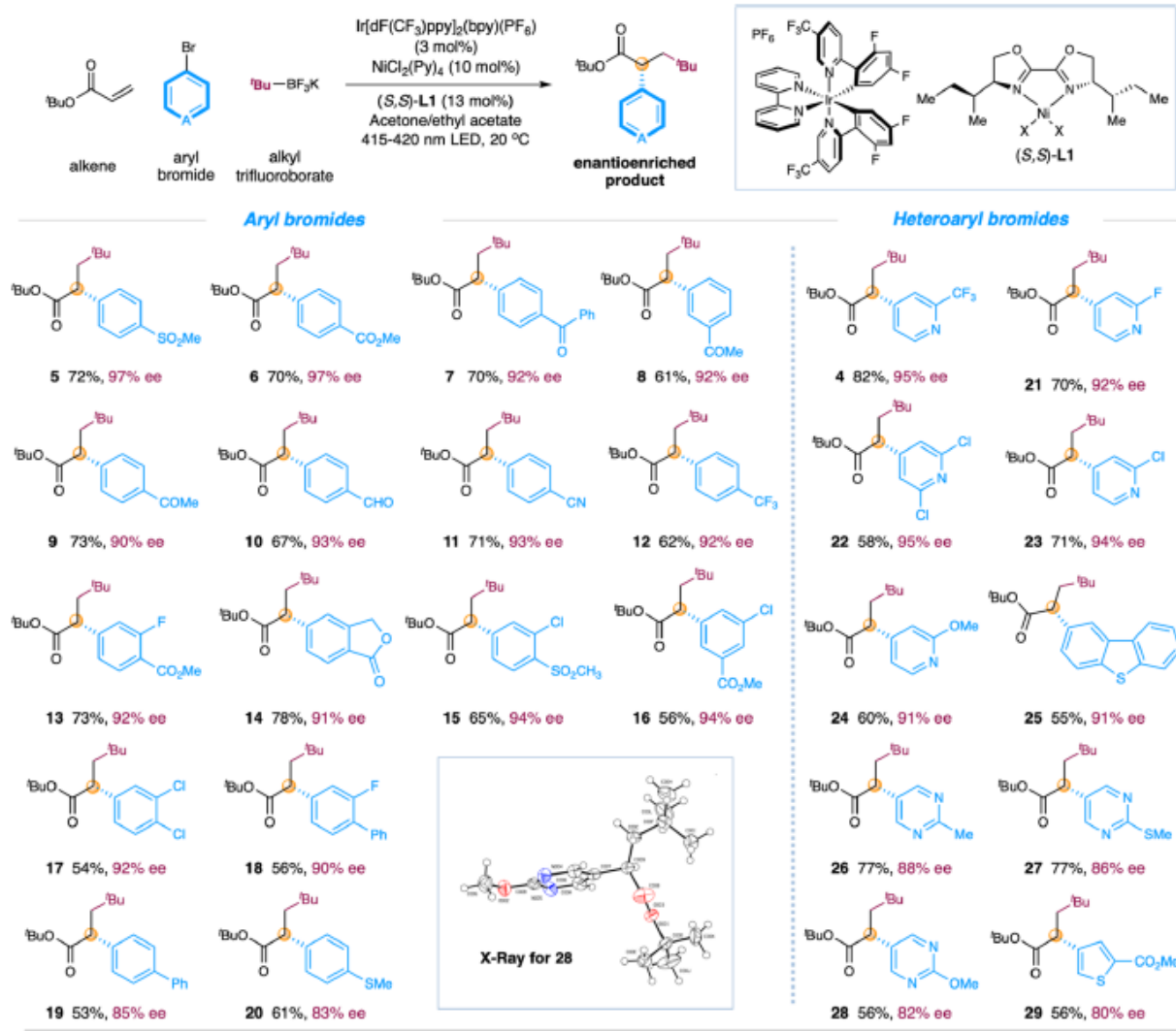


Part III: General Method for Enantioselective Three-Component Carboarylation of Alkenes Enabled by Visible-Light Dual Photoredox/Nickel Catalysis

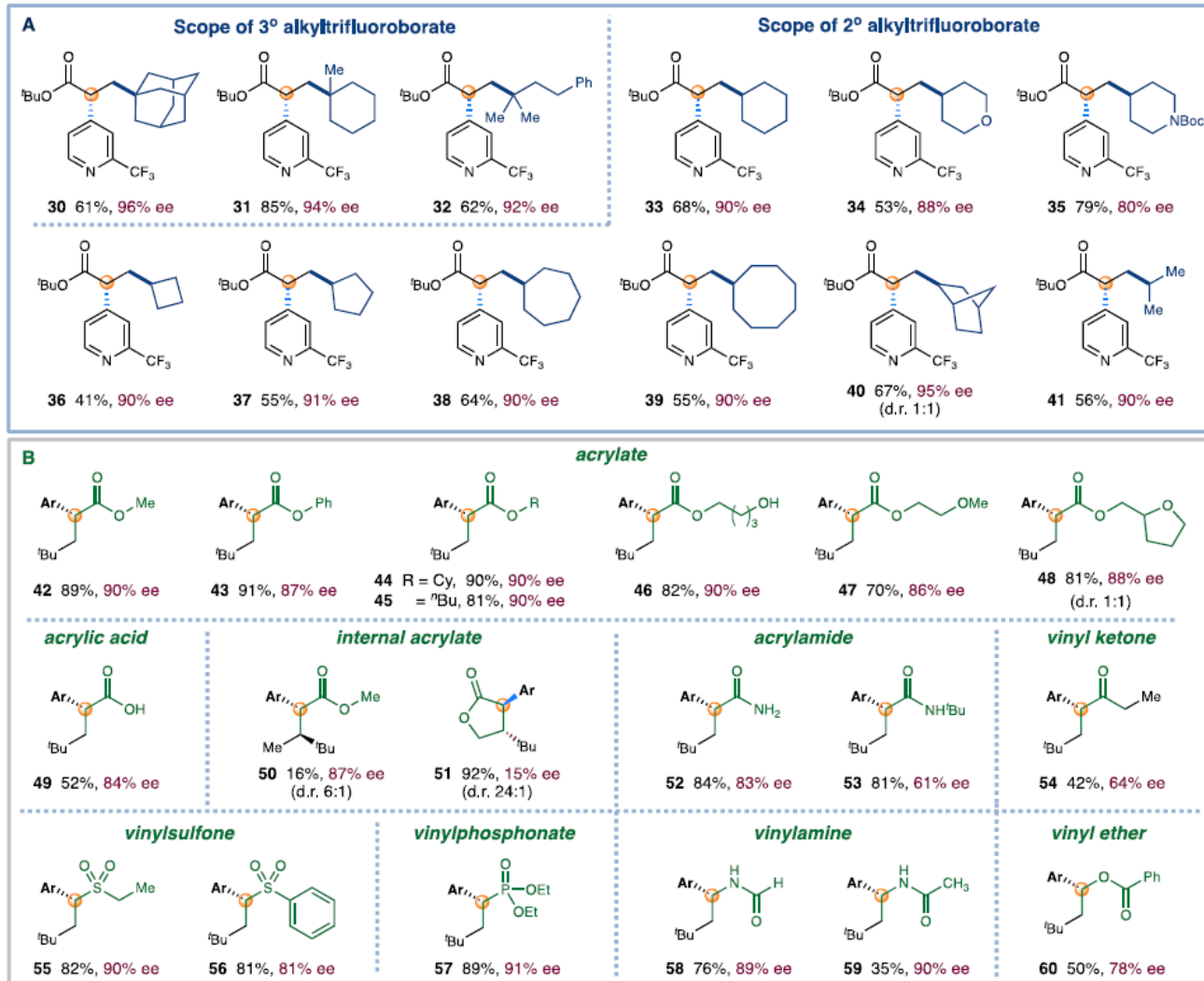


Entry	Variations from the “standard conditions”	Yield	ee
10	10 °C, instead of 20 °C	80%	95%
11	w/o [Ir], [Ni], <i>(S,S)-L1</i> , or light	0%	--
12	$^t\text{BuOCOCO}_2\text{Cs}$, instead of 3	trace	--

Introduction



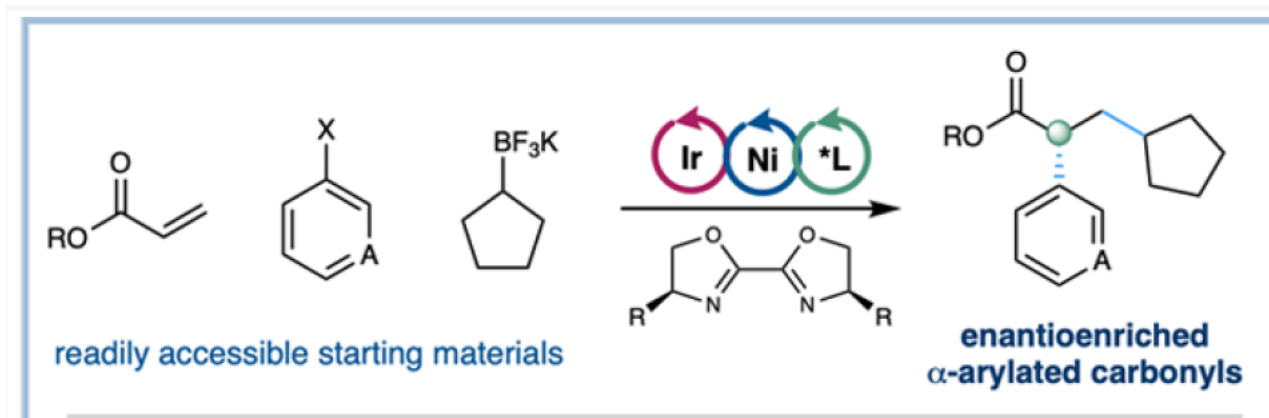
Introduction



Introduction



Part III: General Method for Enantioselective Three-Component Carboarylation of Alkenes Enabled by Visible-Light Dual Photoredox/Nickel Catalysis

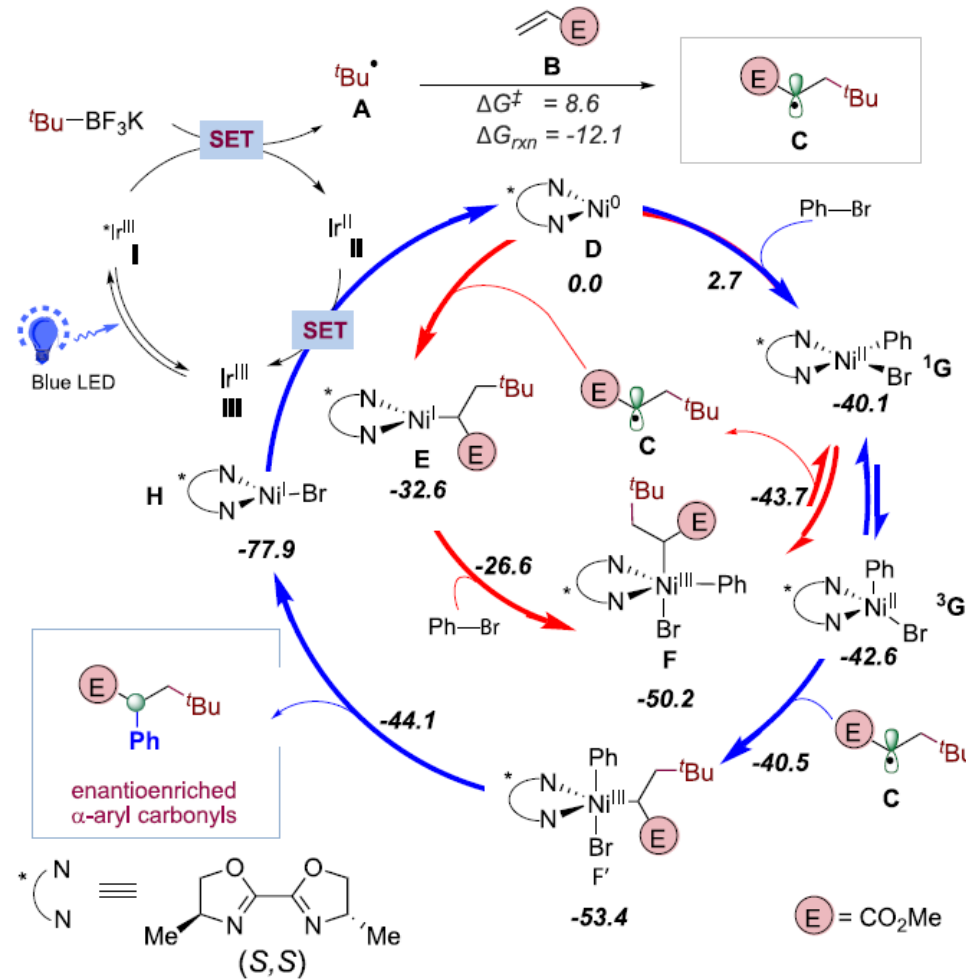


- the factors controlling the regioselectivity;
- the factors controlling the **enantioselectivity**;
- the preference of the three-component carboarylation over the direct arylation of the generated alkyl radical(**chemselectivity**).

Introduction



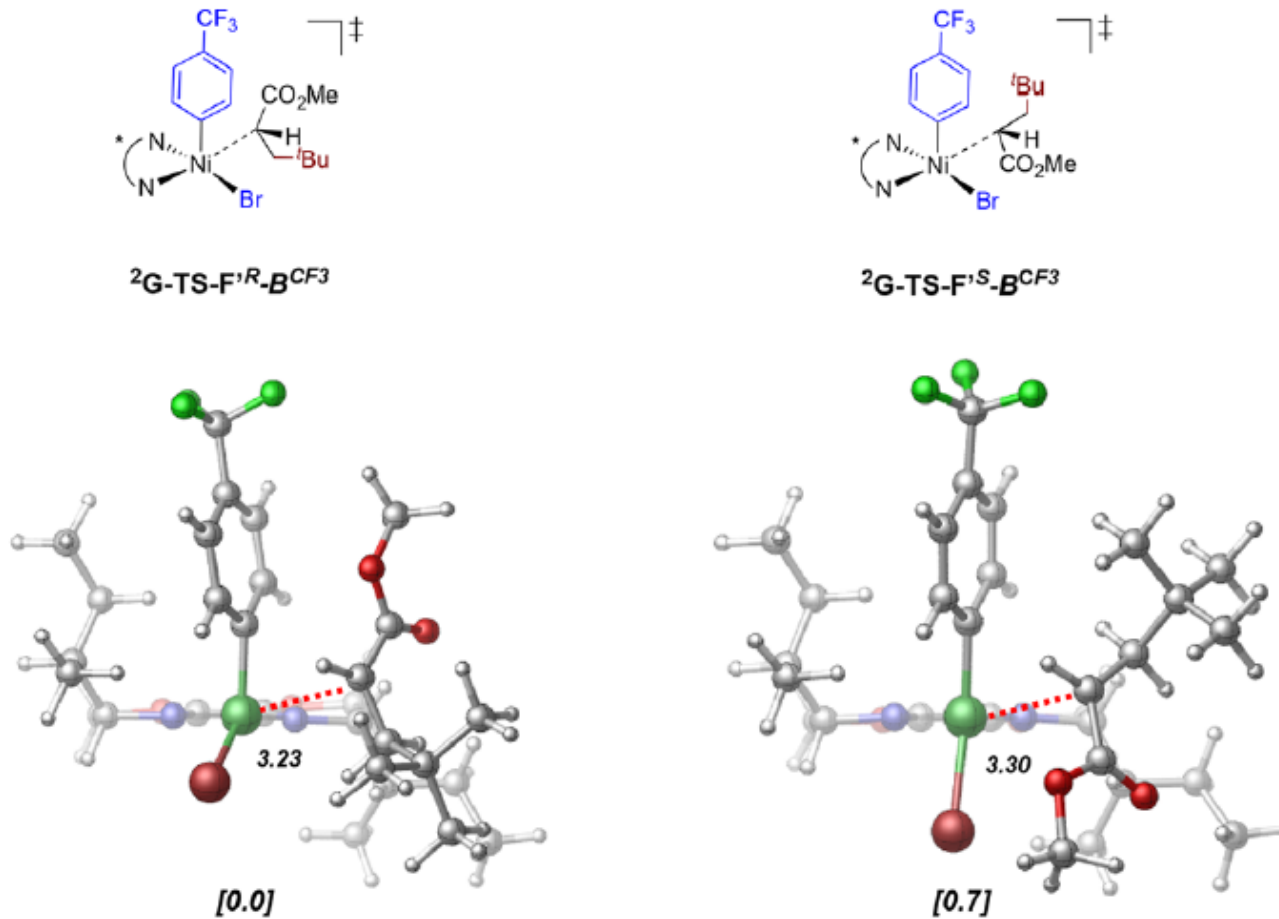
Part III: General Method for Enantioselective Three-Component Carboarylation of Alkenes Enabled by Visible-Light Dual Photoredox/Nickel Catalysis



Introduction



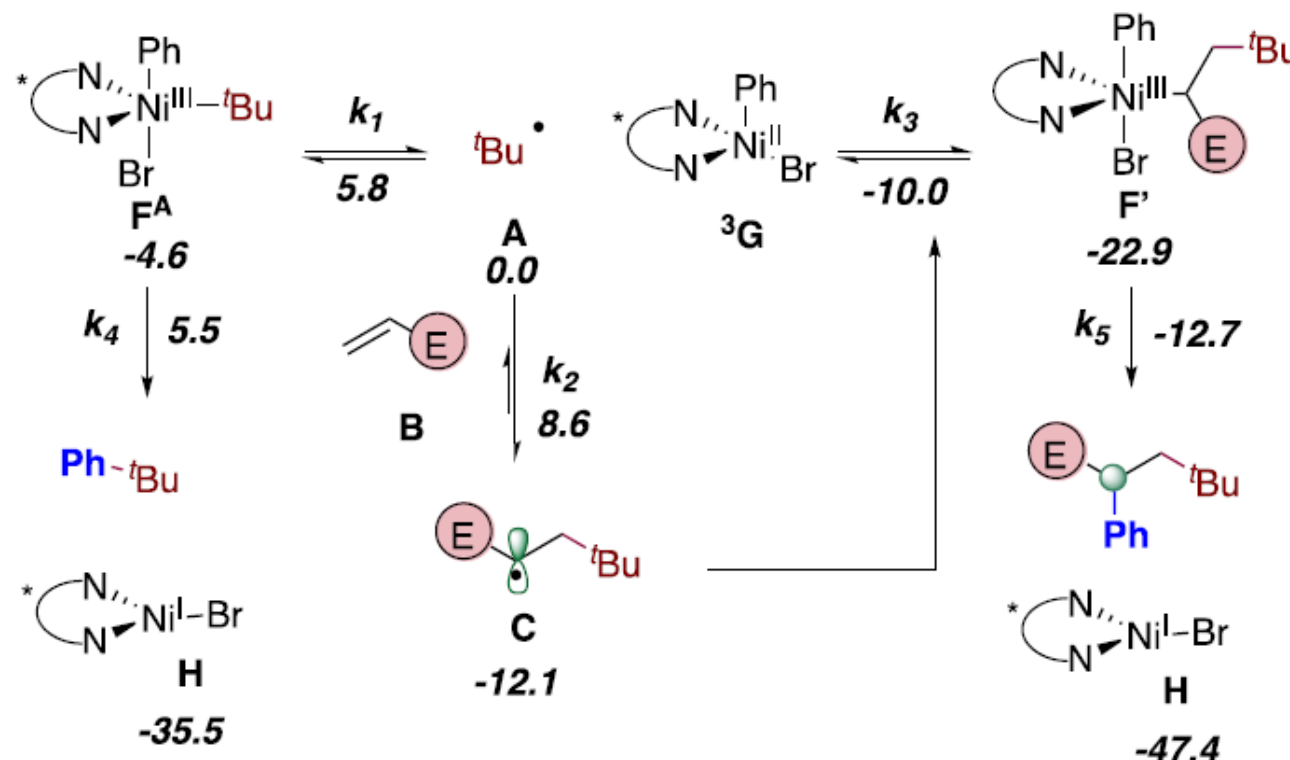
Part III: General Method for Enantioselective Three-Component Carboarylation of Alkenes Enabled by Visible-Light Dual Photoredox/Nickel Catalysis



Introduction



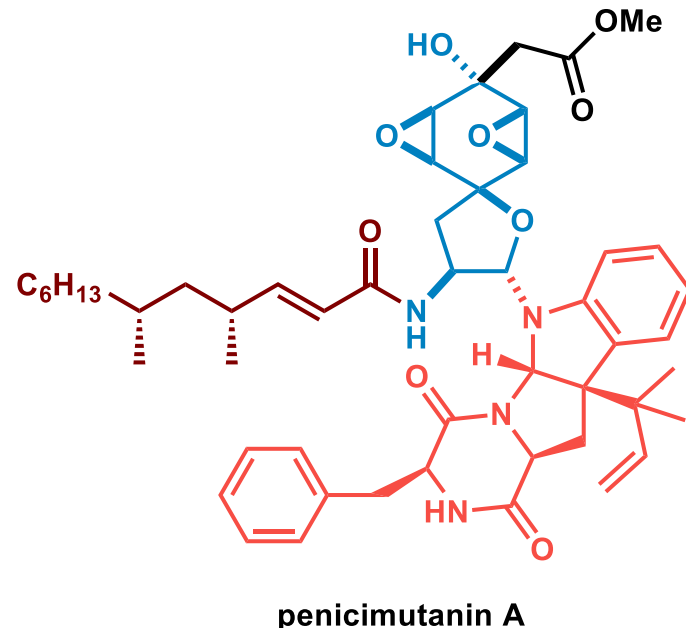
Part III: General Method for Enantioselective Three-Component Carboarylation of Alkenes Enabled by Visible-Light Dual Photoredox/Nickel Catalysis



Origin of Chemoselectivity of the Model System



Total synthesis of (-)-penicimutanin A and Related congeners



Contents



1

Introduction

2

Retrosynthetic Analysis

3

Synthetic Route

4

Summary

Introduction



Tao Xu

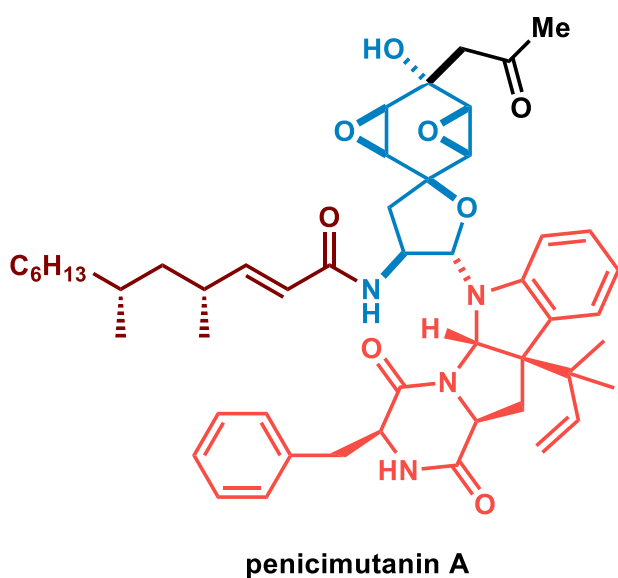
Education & Current job:

- Ph.D.: 2011, Peking University
- Postdoctoral Fellow: 2015, University of Texas at Austin
- Professor: 2015-now, Ocean University of China

Research Interests & Areas:

- ⊕ Natural Product Synthesis
- ⊕ Complex ring system structure methodology

Introduction



Isolation

- Penicimutanin A, isolated from a marine-derived fungal strain identified as *Penicillium purpurogenum* G59 in 2018.

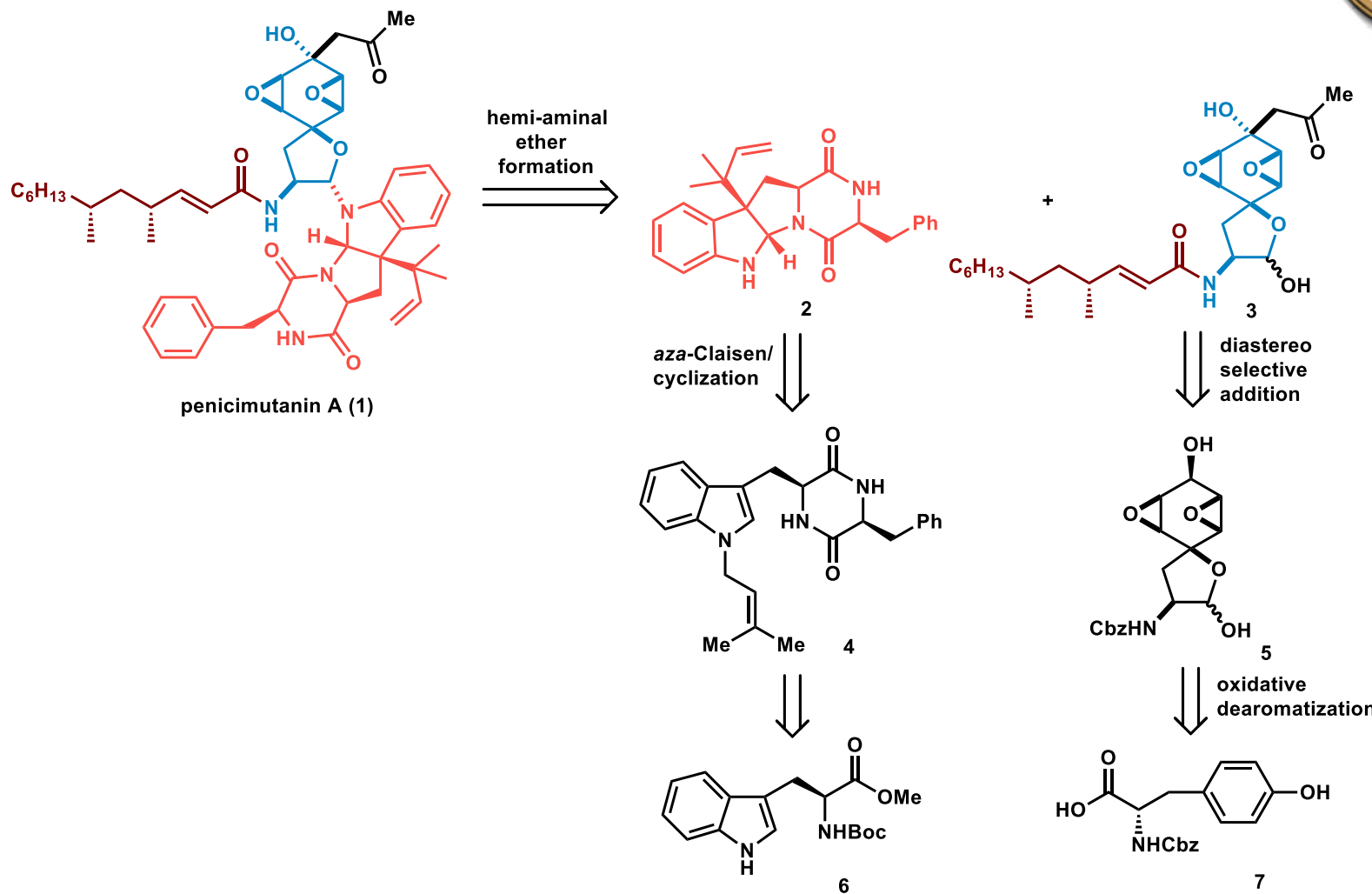
Biological activities:

- Penicimutanin A demonstrated *in vivo* antitumor activity in murine sarcoma HCT116 tumor-bearing Kunming mice.

Structural features

- Labile C2 hemi-aminal ether.
- Diketopiperazine fused hexapyrroloindoline.
- Fully oxygenated cyclohexane ring contains an acid/base-sensitive cis-bisoxirane moiety.

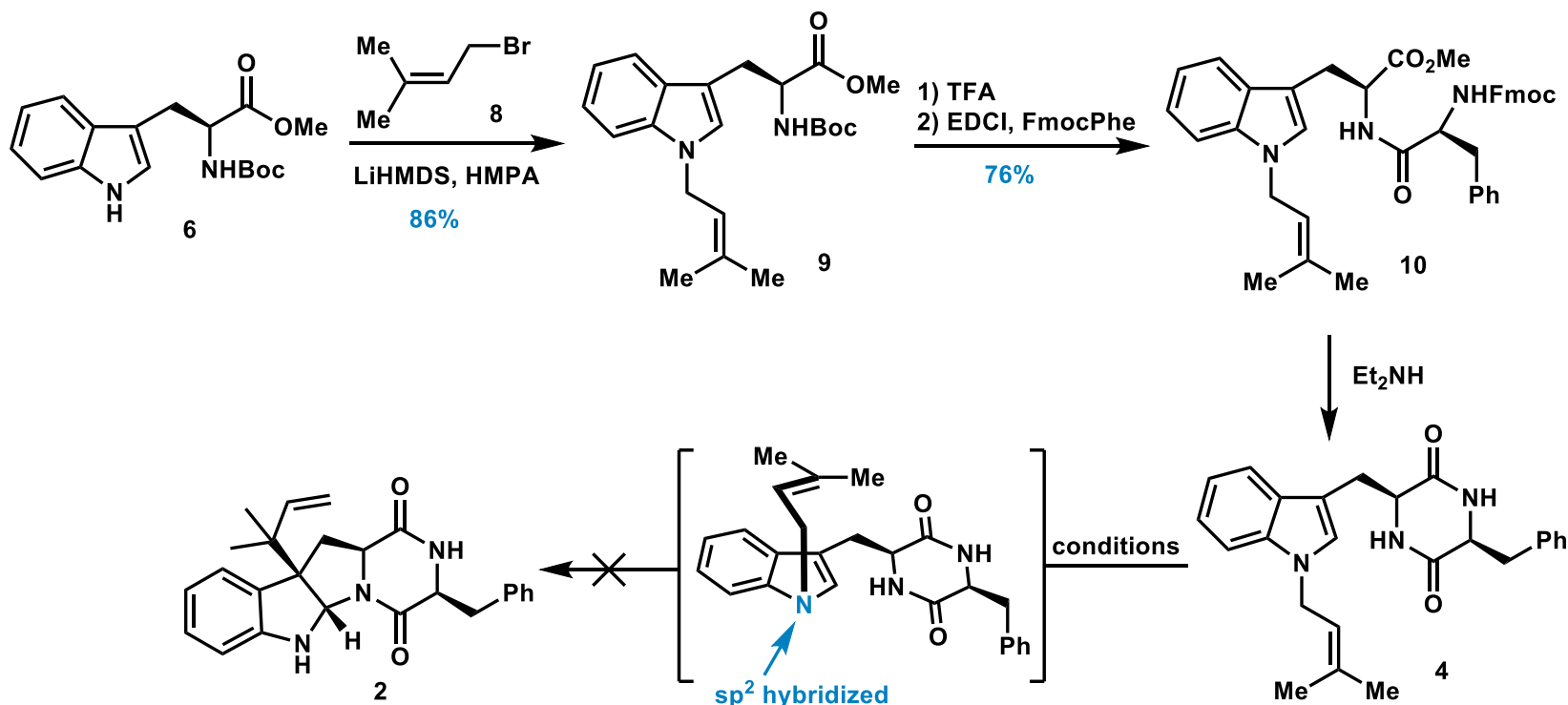
Retrosynthetic Analysis



Synthetic Route



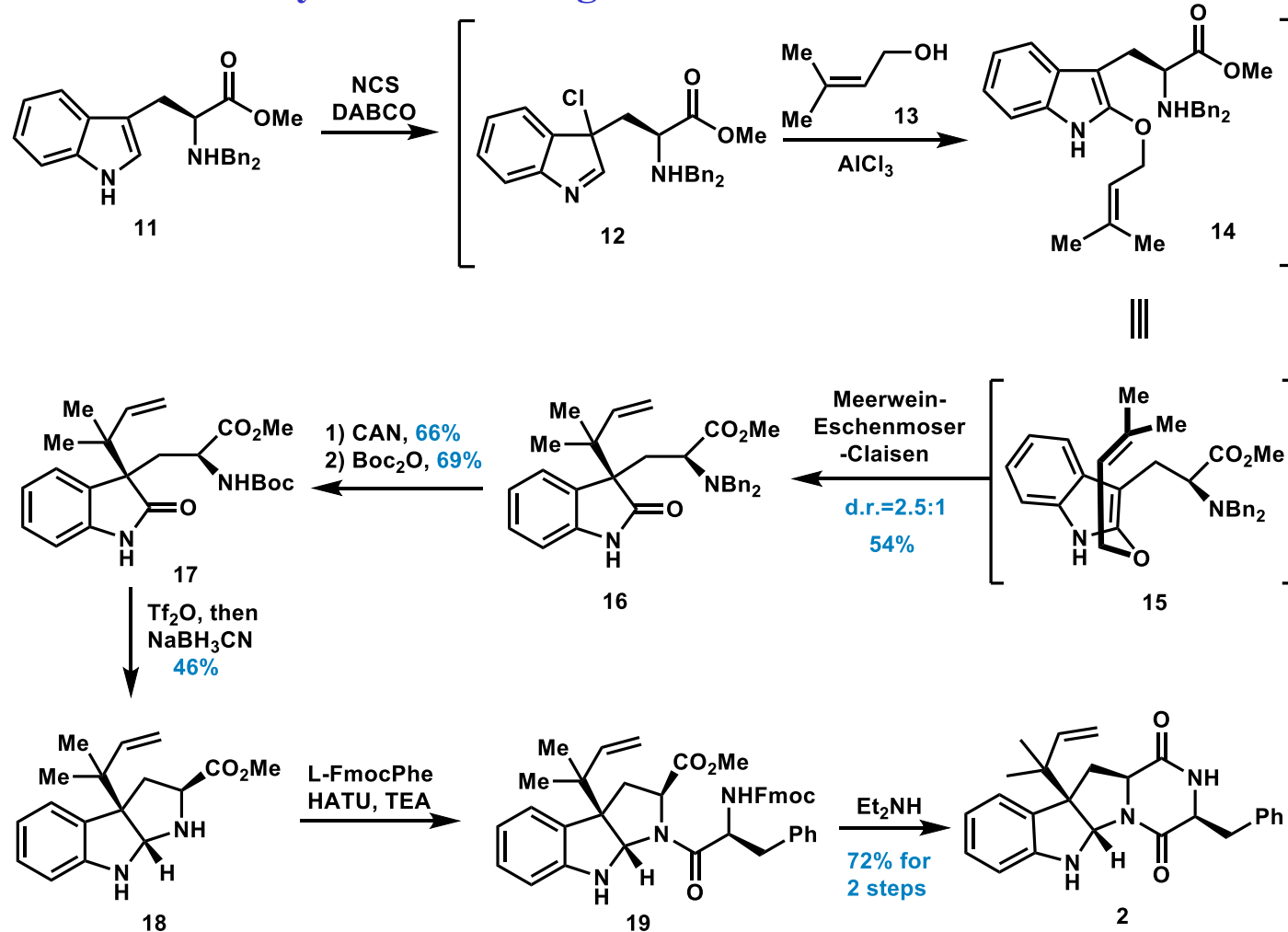
1st generation Route of Synthesis of Fragment 2



Synthetic Route



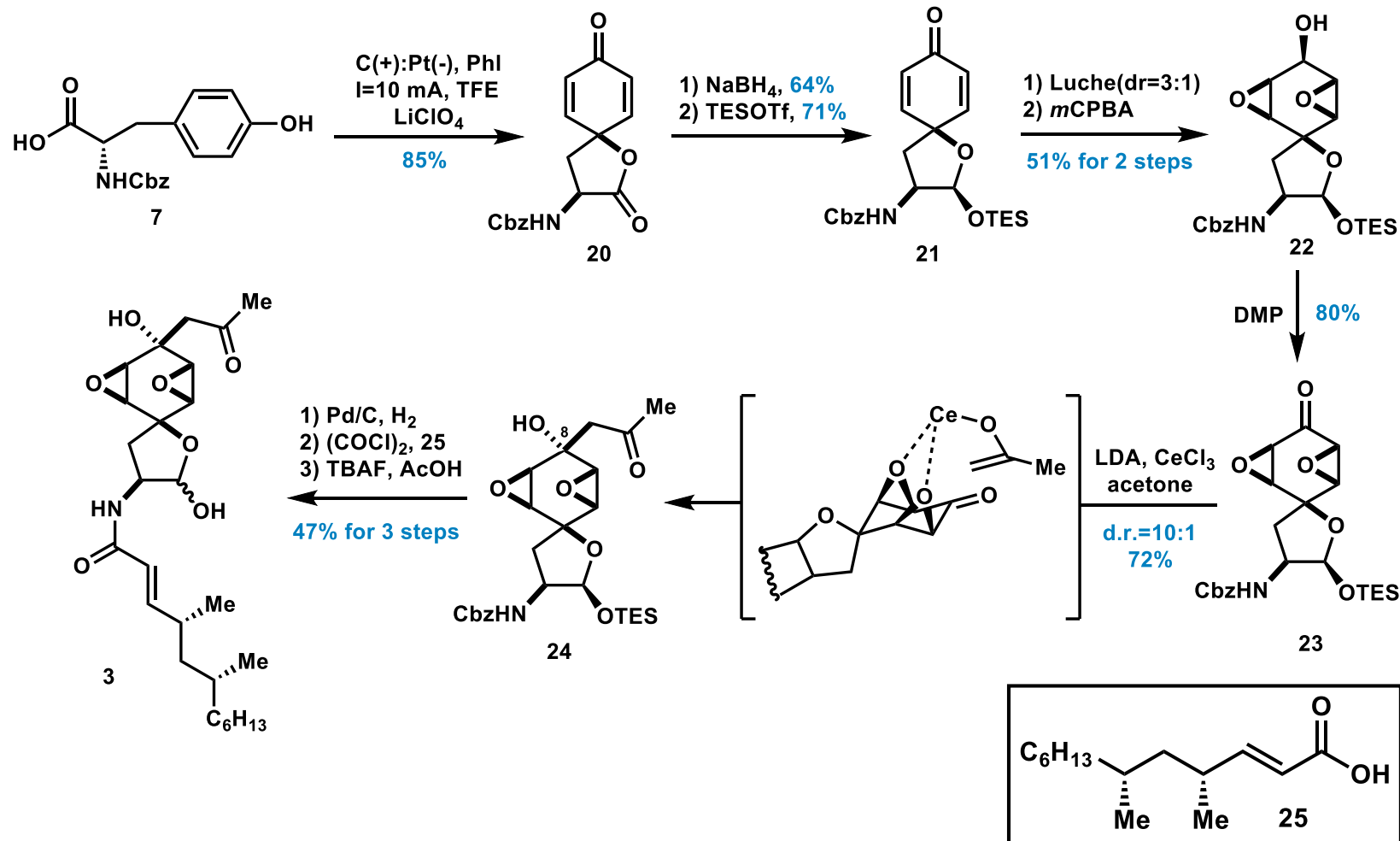
2nd generation Route of Synthesis of Fragment 2



Synthetic Route



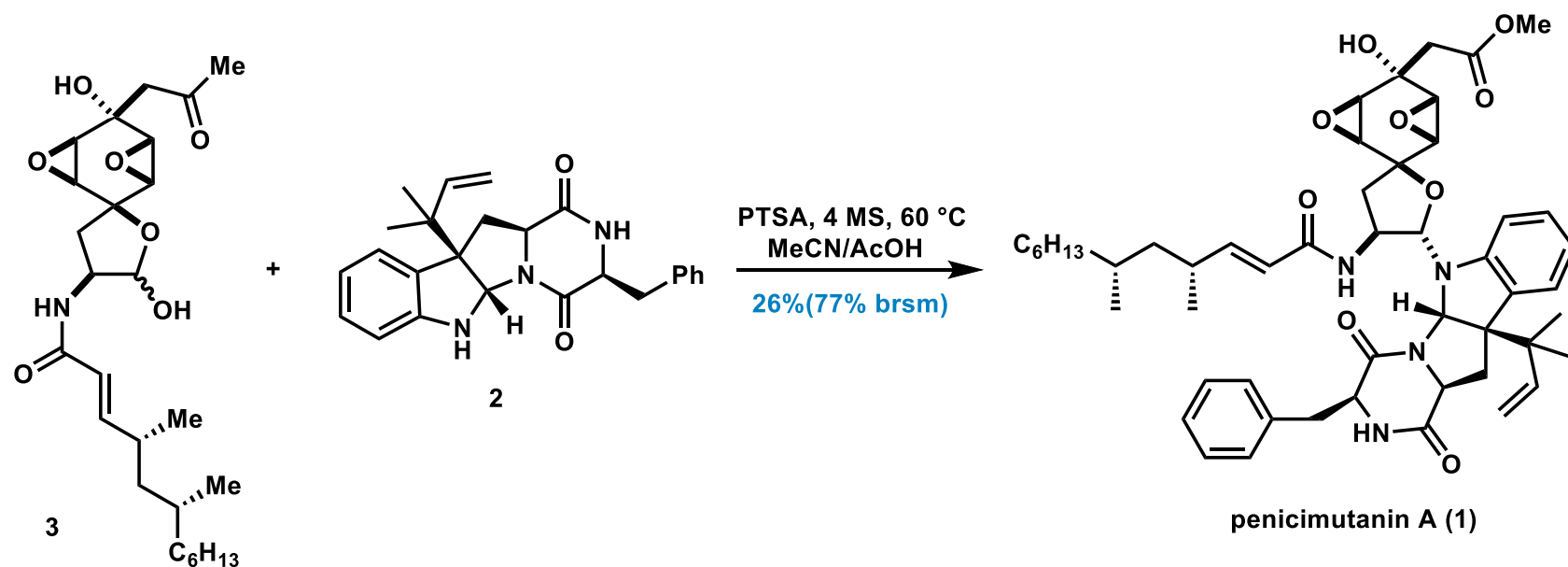
Synthesis of Fragment 3



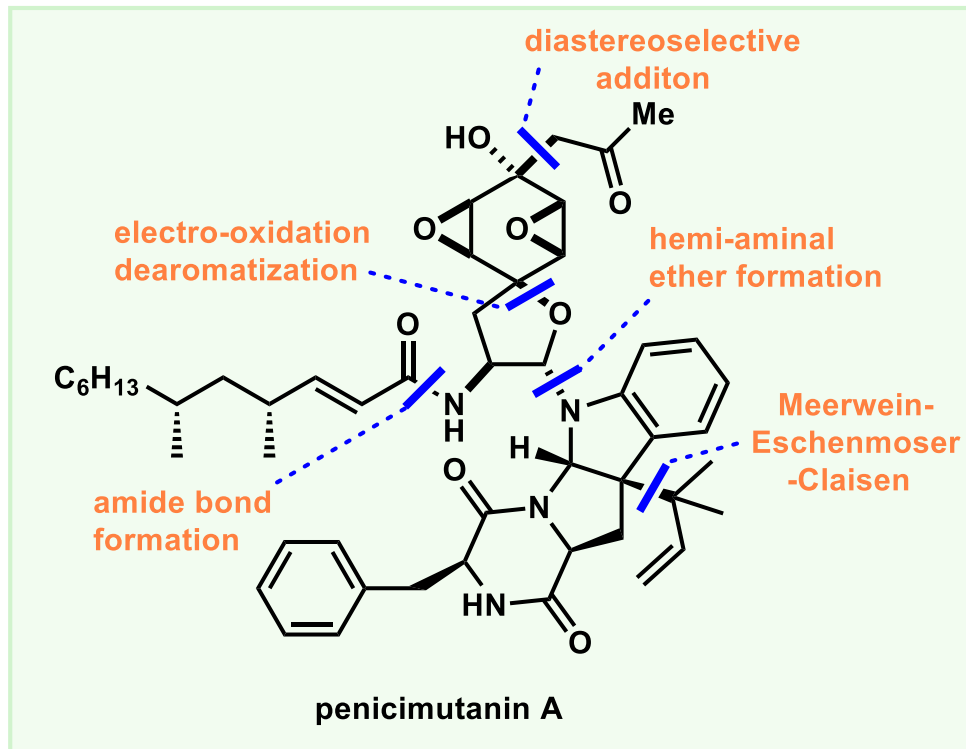
Synthetic Route



Completed total Synthesis of penicimutanin A



Summary



longest liner 10 steps

The End



Thanks for your attention!

Acknowledgement

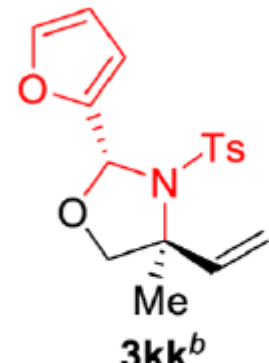
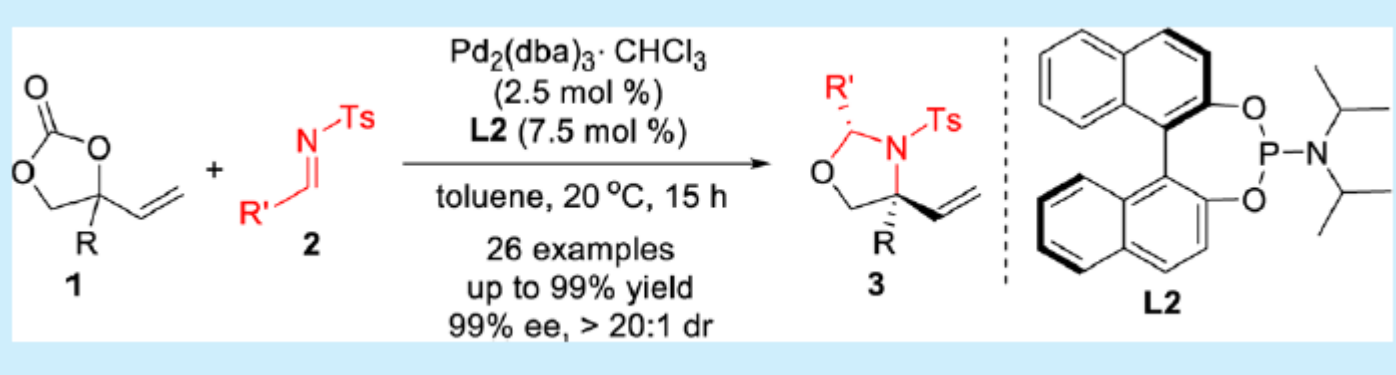


Prof. Tao Ye and Dr. Yi-an Guo;

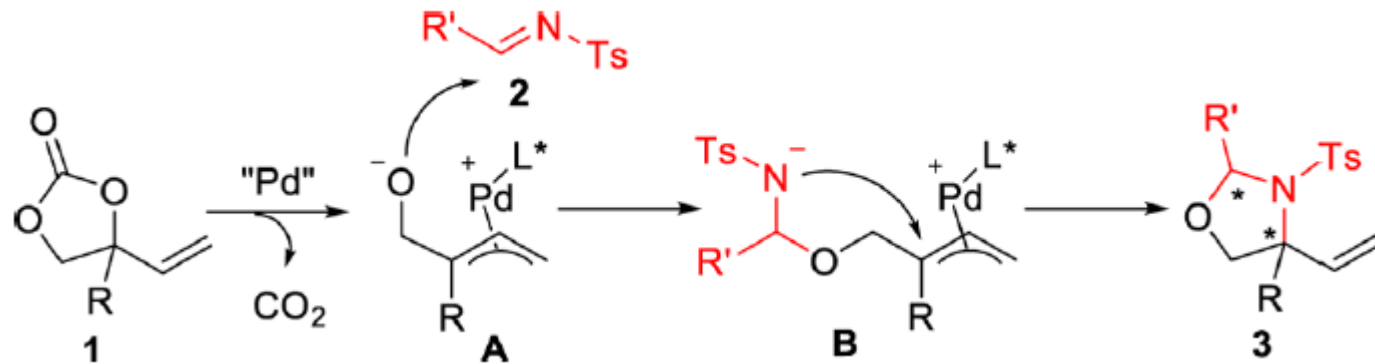
All professors and faculties in SCBB;

All my labmates in F211!

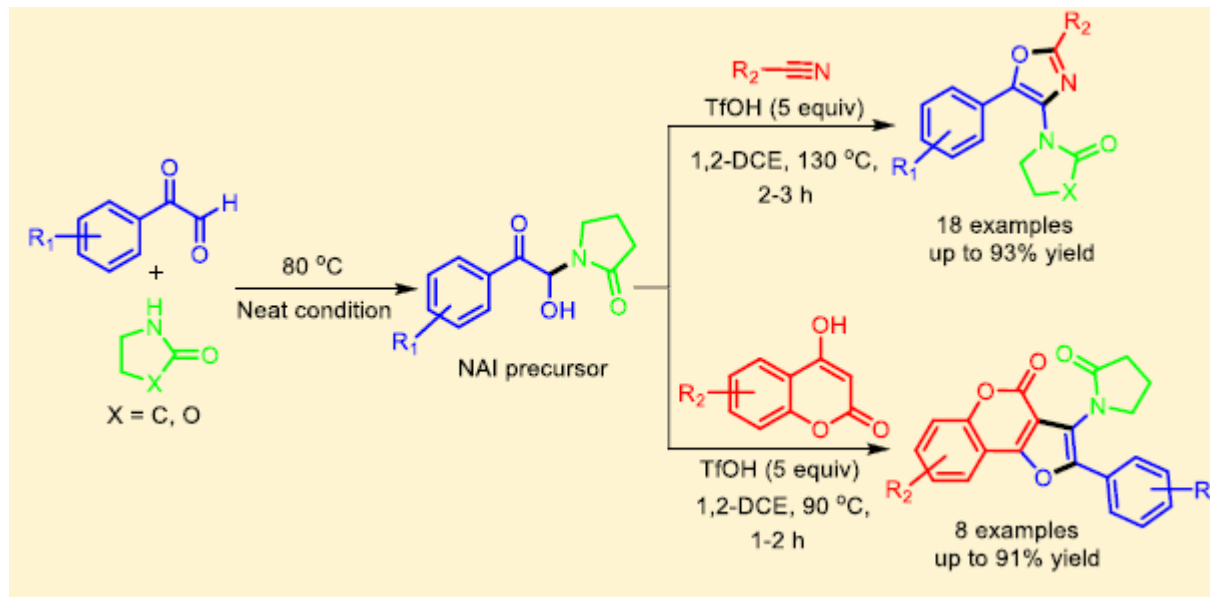
Synthetic Route



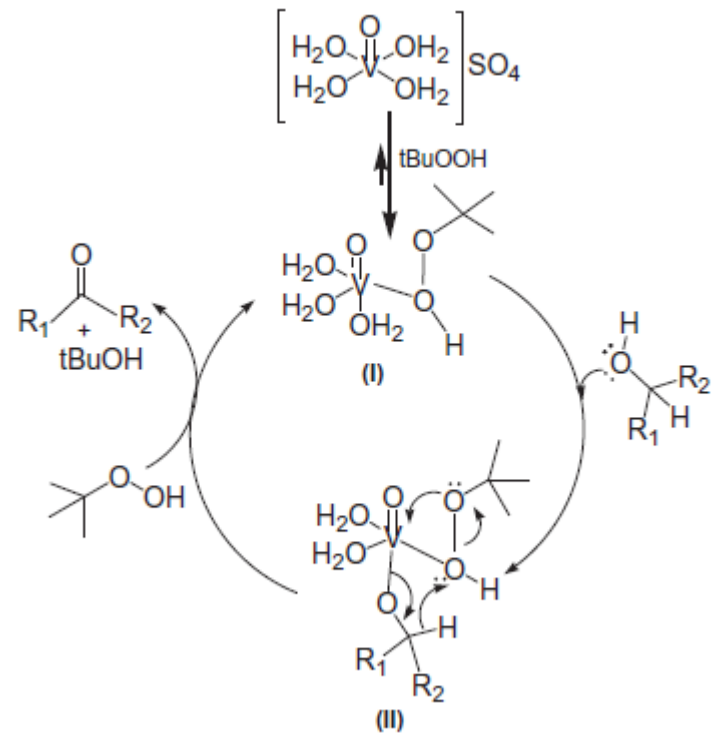
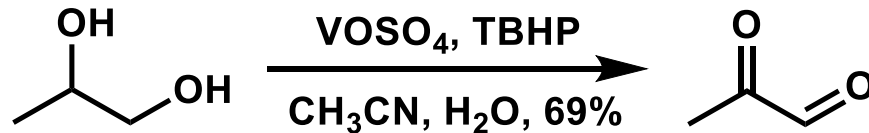
60% yield
10:1 dr, 70% ee



Synthetic Route



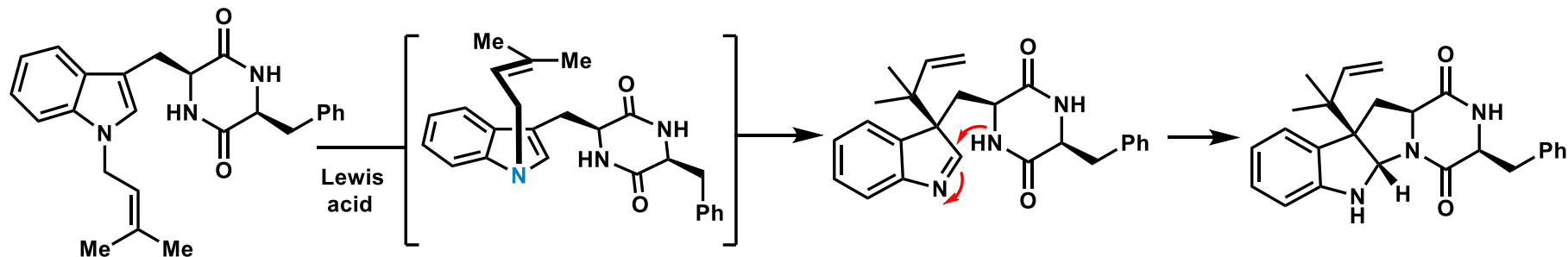
Synthetic Route



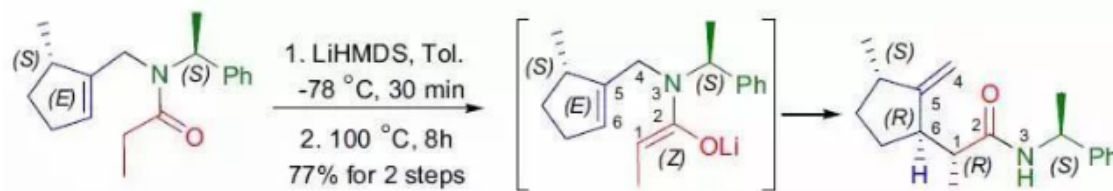
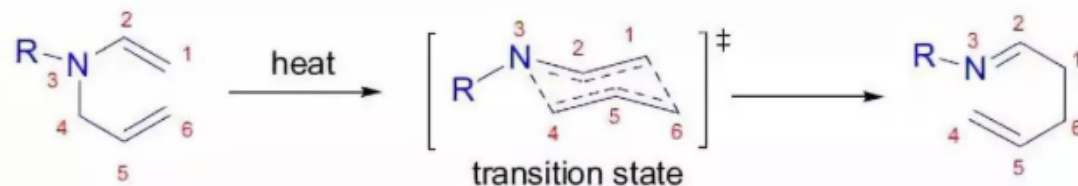
Supporting Materials



Aza-Claisen/cyclization



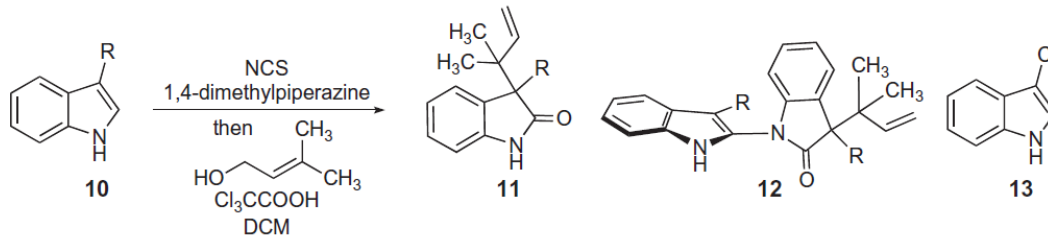
底物通过一个椅式过渡态（胺上的取代基处于平伏键），进行[3,3]- σ 迁移得到产物。



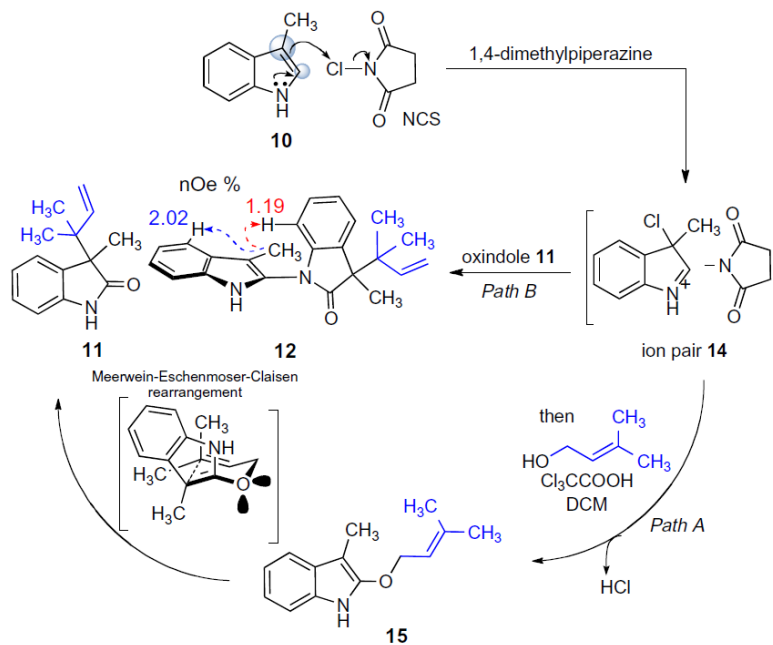
Supporting Materials



Meerwein–Eschenmoser–Claisen rearrangement

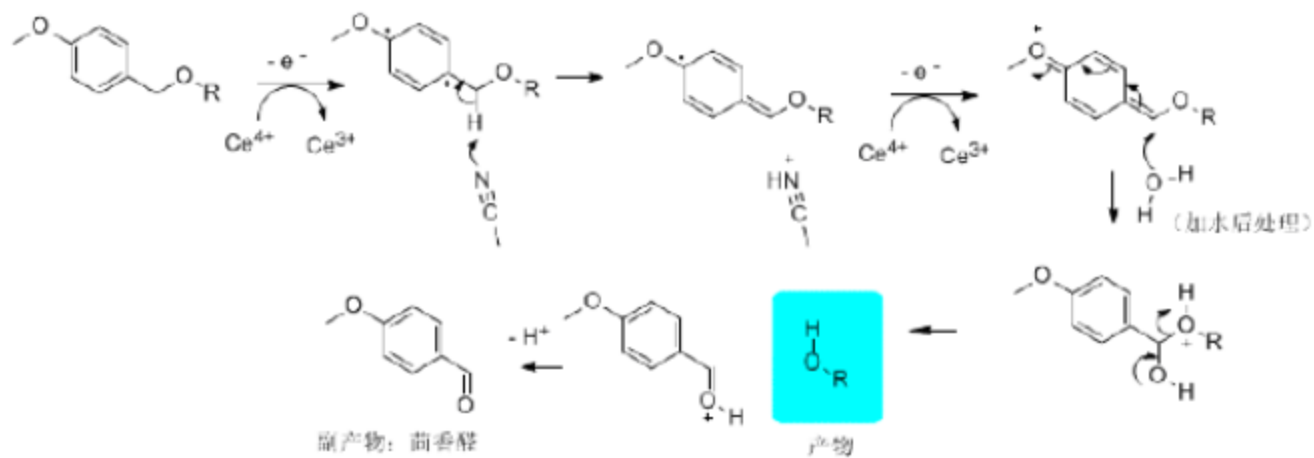


Entry	C3 substitution	% Yield of 11 ^a	% Yield of 12 ^a	% Yield of 13 ^a
1	R = H only 3-chloroindole formed	nd ^b	nd	Quant.
2	R = CH ₃	37.7	2.6	nd
3	R = CH ₂ CH ₂ NPhth ^c	85	nd	nd
4	R = CH ₂ CH ₂ N(CH ₃)NOS ^d	74	nd	nd



were replaced by a hydrogen, which can be lost as a proton to the media, the corresponding ion pair will result in 3-chloroindole **13**. However, in the absence of a C3 proton, dimethylallyl alcohol reacted with this ion pair and caused an addition to occur, leading to, a precursor for an ensuing Meerwein–Eschenmoser–Claisen rearrangement, after the loss of an equivalent of HCl (*path A*). In our experience and of others, this allyloxyimide **15** was transforming immediately even at ambient temperature into its corresponding rearranged oxindole product **11**. The primary driving force for this thermodynamically driven downhill process is accountable based on the fact that an amide bond is generated in the event. In contrast, if the ion pair **14** is encountering the oxindole **11** itself as a nucleophile, especially promoted in the presence of basic components in the reaction mixture, the mechanistic cascade is projected to lead to formation of a different oxindole **12**.¹² In the case of C3 methyl substitution, this dimeric adduct was indeed observed, albeit in low conversion, and was structurally characterized using

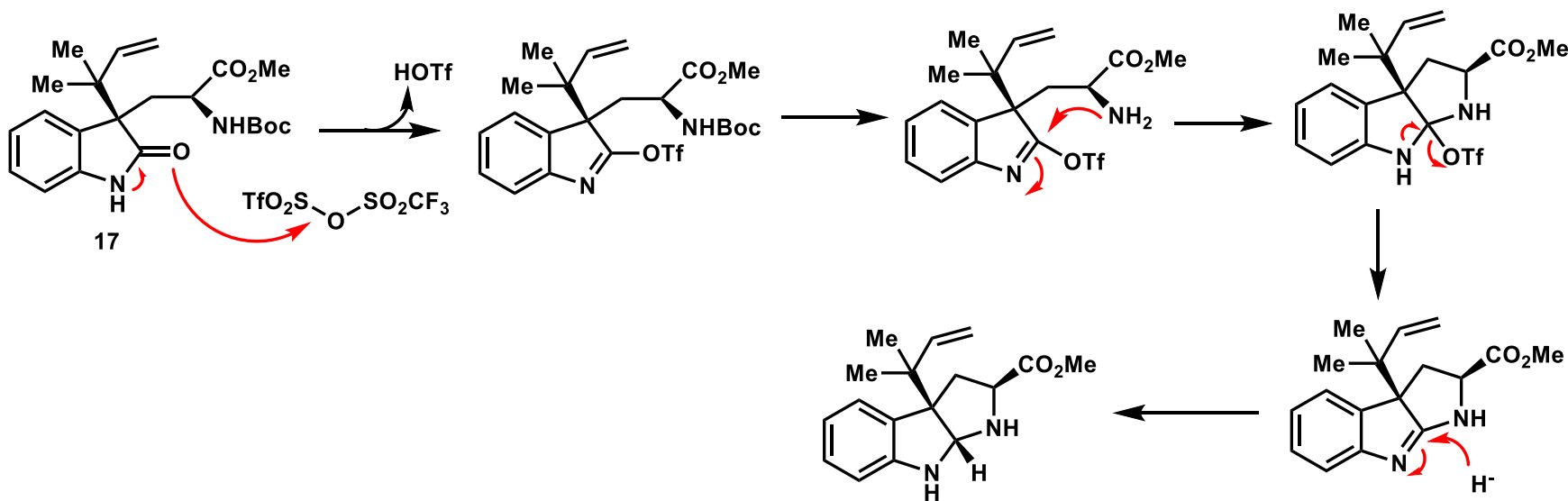
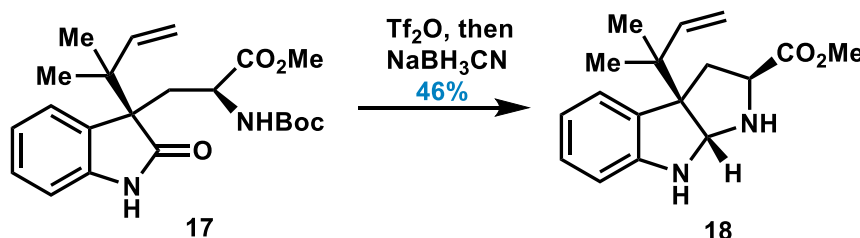
Supporting Materials



Supporting Materials



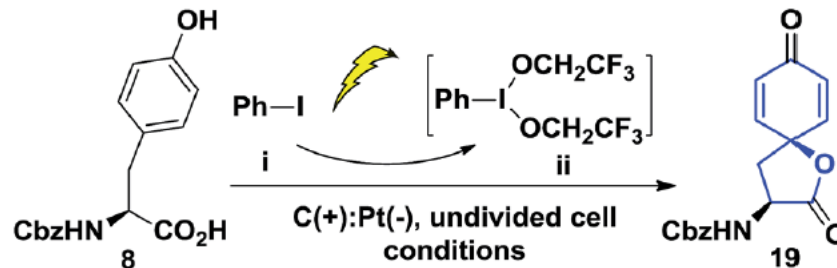
reductive amination



Supporting Materials



oxidative dearomatization



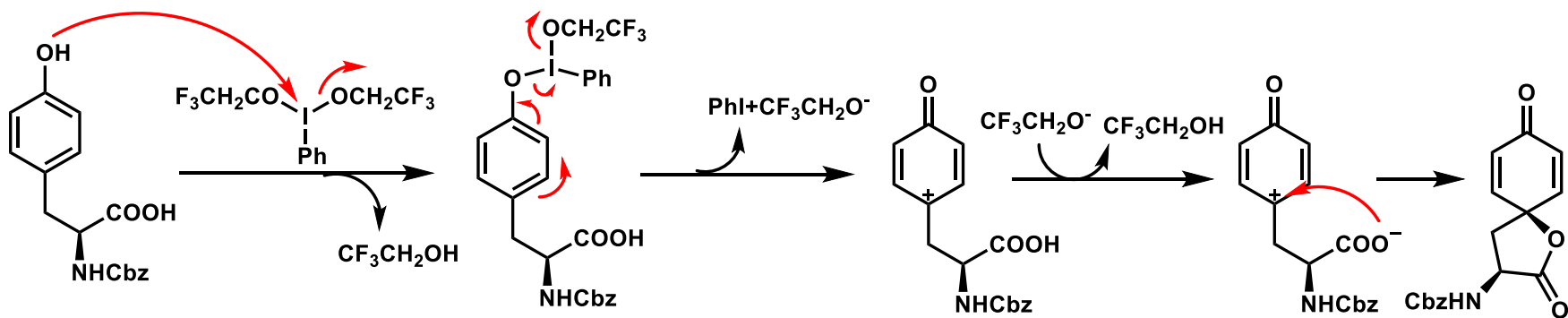
Entry ^a	Conditions	Time	Yield ^b (%)
1	LiClO ₄ (1 eq.), I = 2.1 mA, PhI (1 eq.)	8 h	38
2	LiClO ₄ (10 eq.), I = 6.1 mA, PhI (4 eq.)	4 h	64
3	LiClO ₄ (10 eq.), I = 6.1 mA, PhI (4 eq.)	6 h	65
4	LiClO ₄ (13 eq.), I = 10 mA, PhI (5 eq.)	6 h	65
5	LiClO ₄ (15.6 eq.), I = 10 mA, PhI (6 eq.)	3 h	65
6 ^c	LiClO ₄ (13 eq.), I = 10 mA, PhI (5 eq.)	4 + 6 h	82
7 ^d	LiClO ₄ (15.6 eq.), I = 10 mA , PhI (6 eq.)	5 + 5 h	85

^a All reactions were run with LiClO₄ as the electrolyte, PhI as the additive and a C(+) / Pt(–) anode in an undivided cell on a 0.31 mmol scale using 2,2,2-trifluoromethylmethanol (TFE) as the solvent at a concentration of 0.04 M at ambient temperature for indicated hours with a constant electrical current unless otherwise noted. ^b Isolated yields. ^c The electrical current was stopped after 4 h but stirring was continued for 6 h. ^d The electrical current was stopped after 5 h but stirring was continued for 5 h.

Supporting Materials



oxidative dearomatization



Supporting Materials

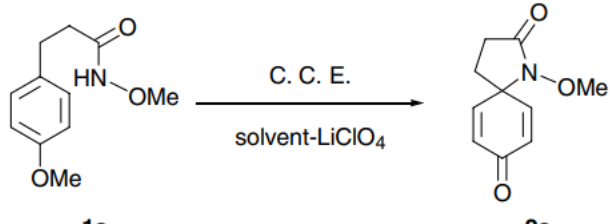


oxidative dearomatization

6506

Y. Amano, S. Nishiyama / Tetrahedron Letters 47 (2006) 6505–6507

Table 1. Direct anodic oxidation of methoxyamide **1a**



Entry	Solvent	Product (%)
1	MeOH	12
2	TFE	67
3	MeNO ₂	32
4	MeCN	16

Anode: glassy carbon beaker, cathode: platinum wire, CCE, 2.5 F/mol.

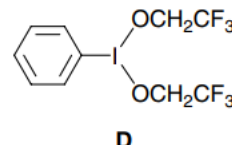
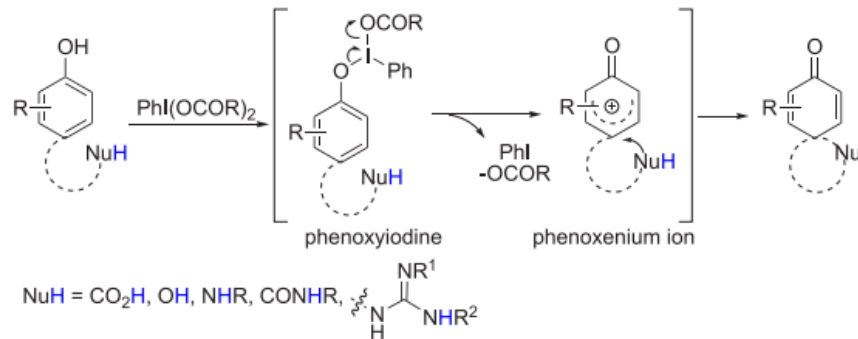


Figure 1. A plausible structure of the oxidant **D**.

unidentified; however, the hypervalent structure **[D]** was conceivable, based on the report of similar iodobenzene derivatives generated under electrolytic conditions⁵ (Fig. 1). In addition, the mixture was submitted to EI mass spectroscopy, which revealed a fragment ion at *m/z* 303 ($\text{PhIOCH}_2\text{CF}_3^+$). A similar ion, *m/z* 317 ($\text{PhIO}_2\text{CCF}_3^+$), was also observed in the EI mass of PIFA.

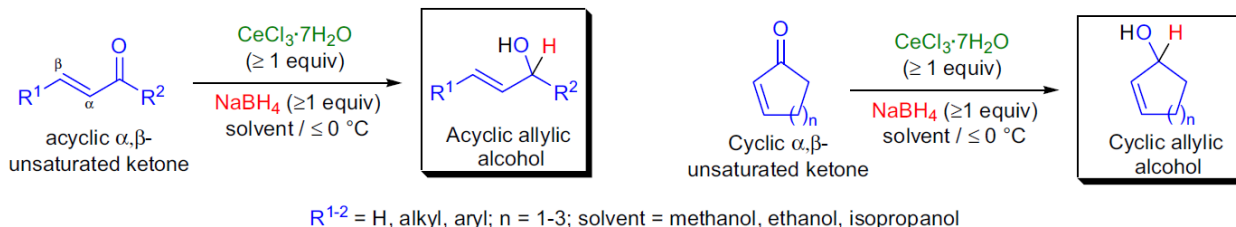
A. mechanism of spirocyclization



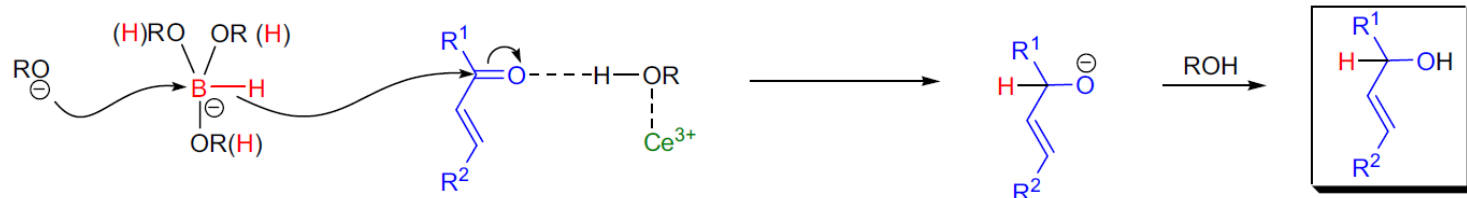
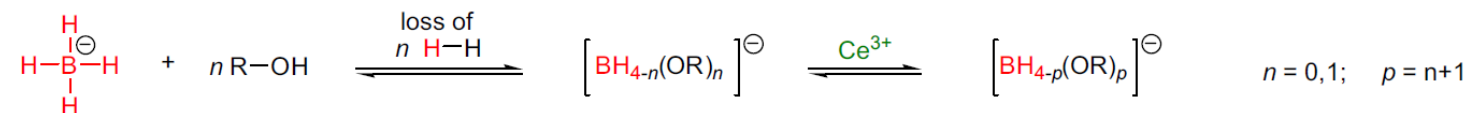
Supporting Materials



LUCHE REDUCTION



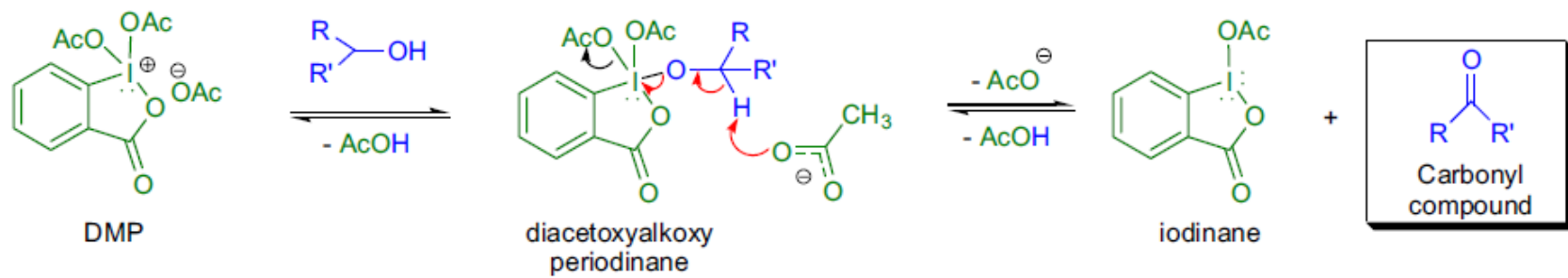
Formation of alkoxyborohydrides:



Supporting Materials



DESS-MARTIN OXIDATION



Supporting Materials



Removal of the PMB ether

